Crystal Orientation Analysis of Injection-Molded Polypropylene by Micro-Beam Wide Angle X-ray Diffraction

Yukihiro Ikura[*1], *Suzune Ito*[*1], *Hirokazu Sasaki*[*2]

ABSTRACT Toward the injection molding specimens which are made of Polypropylene Grafted with Maleic Anhydride melt-blended in polypropylene, we performed the analysis of the crystal orientation in the local region of the specimens with the micro-beam wide angle X-ray diffraction measurement which has a high resolution of Super Photon ring-8 GeV (SPring-8) and is considered with the physical property. As a result, the skin layer of the molding becomes thinner with the influence of the fluidity variation caused by an increase of an additive amount of the polypropylene grafted with maleic anhydride into the polypropylene, however it is found that this addition doesn't have considerable effects on the tensile strength and modulus of the molding.

1. INTRODUCTION

Recently many developments of plastic materials such as glass fiber reinforced polypropylene (PP) are performed for the purpose of weight reduction in automobiles. In such developments, the addition of polypropylene grafted with maleic anhydride (Mah-PP) have been used extensively to improve mechanical properties between the PP and the filler to be added such as glass fiber as the reinforced fiber[1]. Usage of the Mah-PP is also known as one technique of strength improvements of cellulose reinforced plastic material which raised the attention recently[2]. Mah-PP usually has a lower molecular weight and viscosity than PP, therefore, if Mah-PP is added to PP, there is a possibility of changes in the fluidity such as Melt Mass-Flow Rate (MFR) and in the crystallization rate of a molding, and it is figured that changes will occur in the degree of the crystallinity and the crystal orientation and also in the physical properties.

The injection molding is widely applied for, as the molding method of resin, from making dumbbell-like specimens in laboratories to manufacturing of large moldings. The injection molding is a manufacturing method that is injecting a molten resin into a mold. When the molten resin is injected into a mold, the surface of the dissolved resin which gets in contact with the mold is cooled rapidly and a skin layer is formed. Since thermal conductivity of the inner region of the plastic is extremely small comparing with that of the metal mold, the inner part of the molding isn't cooled rapidly, therefore it forms a core layer.

[*1] Laboratories for Fusion of Core Technologies, R&D Division
[*2] Advanced Technologies R&D Laboratories, R&D Division

However there are few examples of detailed analysis about variations of crystal condition and others in the injection molding of the PP blended Mah-PP. Therefore, in this study, as a core technology for analysis, on the injection molded specimen consist of a neat PP melt-blended with the Mah-PP, by observing wide angle X-ray profiles of local region in the injection molding using micro-beam X-ray of SPring-8,which has a high resolution, we analyzed the degree of crystallinity and crystal orientation in the thickness direction of the molding, as factors which have influence on the mechanical properties.

2. THE EXPERIMENTS

2.1 Micro-beam Measurement Using Synchrotron Radiation Facility

For the X-ray equipment in the laboratory system, there is a limitation to focus to a beam generally which has a diameter of hundreds micrometers, therefore it is difficult to obtain information from a local region of few micrometers. On the other hand, for the industrial products, the in-plane distribution analysis of products structure with spatial resolution of few micrometer order is often required. The synchrotron radiation facilities such as SPring-8 implement micro-beam in several beam lines to meet such industry's requirements. BL24XU of SPring-8 administered by Hyogo Prefecture brings off to focus with the X-ray to smaller than 10micrometer. Using this micro-beam, Small Angle X-ray Scattering (SAXS) measurement, Wide Angle X-ray Diffraction (WAXD) measurement, or X-ray Absorption Fine Structure (XAFS) analysis can be realized. In this study, from those analysis methods, we took the micro-beam wide angle X-ray diffraction to attempt the crystalline orientation analysis on the PP.

2.2 Micro-beam Wide Angle X-ray Diffraction Measurement and Crystalline Orientation Analysis of PP by Using Synchrotron Radiation Facility

Micro-beam wide angle X-ray diffraction measurement was done by using BL24XU of SPring-8 with 96 mm of camera length. The photograph of the equipment is shown in Figure 1. The measurement condition is that X-ray of 8.2×7.0 μm^2 (FWHM) beam size and 0.12 nm wavelength (10 keV) and PILATUS3-X-300K (487×689 pixels, pixel size 172 μm^2) is used as a detector and the exposure time is set as 5 sec. The measurement is performed scanning at 40 points in the Normal direction (ND) on the Machine direction-Normal direction (MD-ND) plane from the surface to the middle of the thickness of the specimen which is a 1 mm (approx.)-specimen (Figure 2) cut out from the parallel part of 2 mm-thick tensile test specimen.

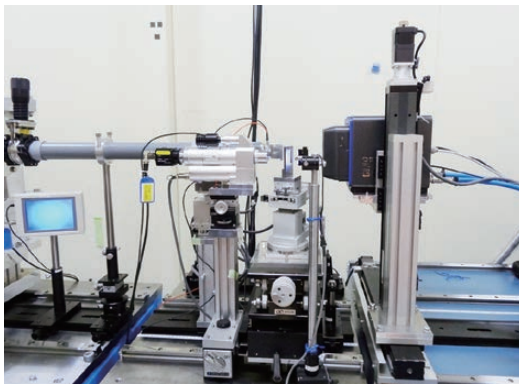

Figure 1 Schematic photograph of micro-beam-WAXD equipment.

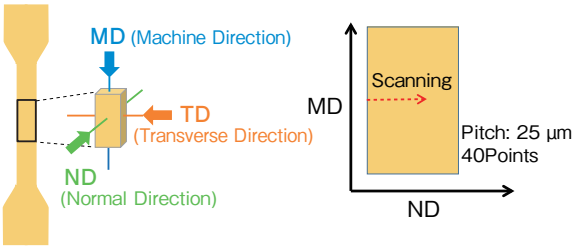

Figure 2 Schematic diagram of the dumbbell specimen MD-ND plane.

According to the diffraction peak position, the crystal structure of the PP obtained from this X-ray diffraction measurement mainly belongs to an α-form. The α-crystal of the PP is monoclinic phase and each lattice parameter are a=0.665nm, b=2.096nm, c=0.650nm and β=99.20°[3]. A representative 2D-WAXD pattern in the skin layer of the PP is shown in Figure 3. The diffraction peaks in the Figure 3 belong each from the center in order to (110)-plane, (040)-plane, (130)-plane and (111)-plane. This time, the (110)-plane is used for the orientation analysis on the PP. The reasons are that sufficient diffraction intensity can be obtained with the diffraction of the (110)-plane, there is a possibility to overestimate the degree of orientation in the c-axis because the orientation information derived from a-axis and c-axis appear at once in the equatorial direction if the (040)-plane is used for the analysis, and also the diffraction peak which belongs to β-crystal's (300)-plane is observed in the slightly inner side of the (040) at some measured locations therefore it is difficult to separate them when the orientation is analyzed.

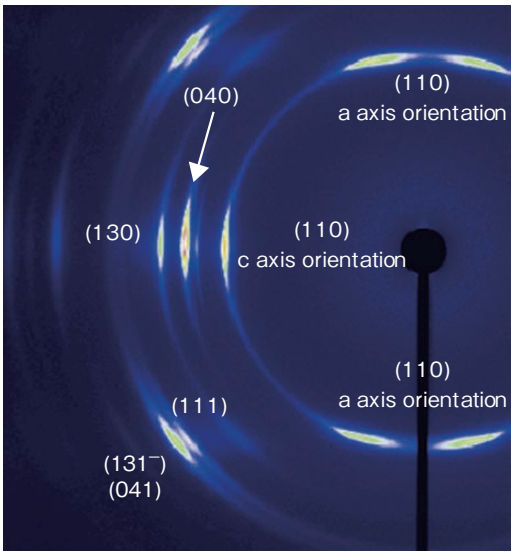

Figure 3 2D-WAXD pattern of surface region of MD-ND plane for a PP injection-molded sample.

The 2D-WAXD pattern of the Figure 3 is shown in Figure 4 as the 1D-WAXD pattern. In the 1D-WAXD pattern of the Figure 4, as "h" is the peak height, "p" is the peak location, "w" is the half-value width and "x" is the angle, we applied curve fitting by using Lorentz function L(x) shown below.

$$L(x) = \frac{h}{1 + \frac{(x-p)^2}{(w/2)^2}}$$

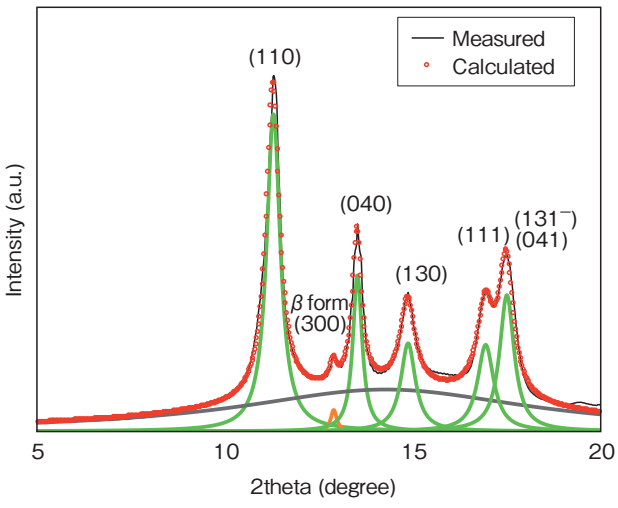

Figure 4 1D-WAXD pattern of surface region of MD-ND plane for PP injection-molded sample.

As the result, the peak location "p" of (110) plane is 2θ=11.3°. Therefore, we used an angle range of 2θ= 10.8° - 11.8° for the orientation analysis and made 1-dimension profile of azimuthal angle (Φ) direction. This 1-dimension profile is shown in Figure 5.

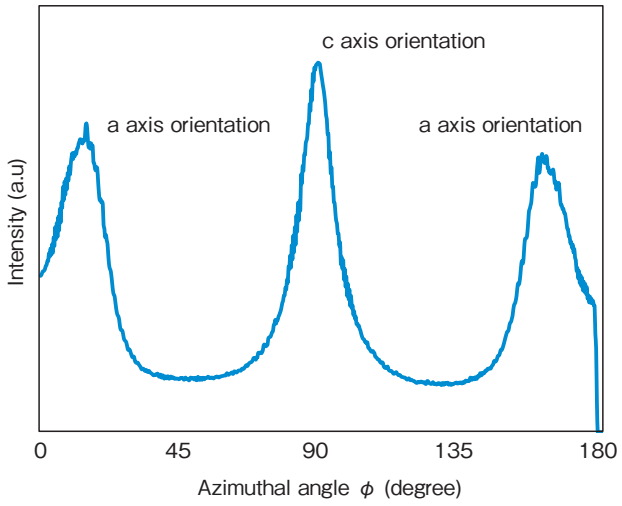

Figure 5 Azimuthal intensity distribution of (110)-plane of a PP crystal.

We used the orientation function f in the following for the analysis of orientation degree.

$$f = \frac{3\langle\cos^2\phi\rangle - 1}{2}$$

$$\langle\cos^2\phi\rangle = \frac{\int I(\phi)\cos^2\phi\sin\phi d\phi}{\int I(\phi)\sin\phi d\phi}$$

Where, $I(\Phi)$ is the intensity profile in the azimuthal angle direction of (110)-plane.

As shown in Figure 5, in the skin layer of the PP, both orientation information of the a-axis orientation (15° and 161°) and the c-axis orientation (90°) are observed at once in the azimuthal angle direction. The higher-order structure is known that it becomes parent-daughter lamellar structure which is parent lamellar with molecular chain arrayed and growing crystal in the flow direction, accompanied by a daughter lamellar with a-axis arraying in the flow direction and growing crystal[5]. In this study, the purpose is to obtain the orientation information of c-axis as the molecular chain, therefore the orientation components of a-axis and c-axis are eliminated by peak resolution and the orientation function f with only the orientation component of c-axis is obtained.

2.3 The Manufacturing of Composition for the Evaluation

Homo-PP (Melt Mass Flow Rate: MFR approx.15 g/10 min) and commercially available Mah-PP are melt-blended as the concentration of the Mah-PP becomes 0, 1 and 3 mass% by using a twin screw extruder. Each blend pellets are obtained by water-cooling and pelletizing from the twin screw extruder.

2.4 The Injection Molding

Dumbbell specimens of each blend pellets which support the standard of JIS No.5 are molded by using electric injection molding machine "ROBOSHOT" α-S301A of FANUC CORPORATION. The cylinder temperature is 200°C and mold temperature is 40°C.

2.5 The Measurement of Melt Viscosity

Melt Mass Flow Rate (MFR) is measured for each blend pellets under the condition of 230°C cylinder temperature and 2.16 kg load by Melt Flow Index Tester of YASUDA SEIKI SEISAKUSHO, LTD.

2.6 The Measurement of Melt Crystallization Behavior

Differential Scanning Calorimetry (DSC) measurement is measured by Thermal Analyzer TA-60A of Shimadzu Corporation. The injection molding specimens for each composition are cut out into approx. 10 mg, filled in an aluminum pan, sufficiently dissolved at the temperature up to 200°C and then the exothermic peak temperature caused by crystallization is measured while cooling them at the cooling rate of 10°C/min.

3. RESULT AND CONSIDERATION

3.1 The Effect of the Mah-PP Addition to the Fluidity and Crystallization Behavior

The DSC thermograph of each blend pellets is shown in Figure 6. As many as the Mah-PP is added, the crystallization temperature shifts to higher temperature and the tendency such that crystallization rate becomes faster is confirmed.

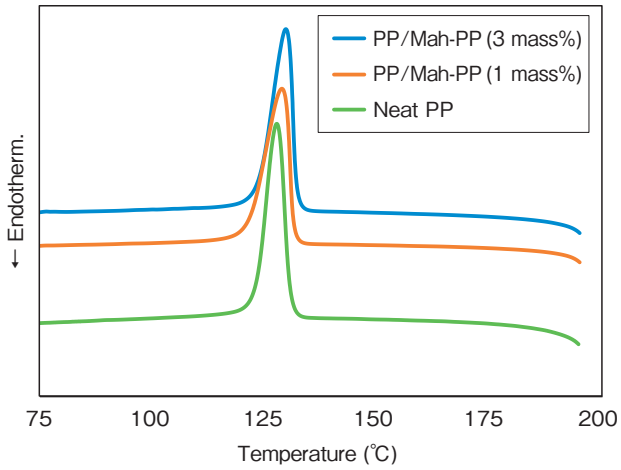

Figure 6 DSC thermograph of cooling curve for neat PP and PP/Mah-PP blends.

The result of MFR measurement is shown in Table 1. MFR becomes lager as many as Mah-PP are added. That is, it is considered that the viscosity decreases as many as Mah-PP are added.

Table 1 Crystallization temperature and MFR of neat PP and PP/Mah-PP blends.

Mah-PP content [mass%]	Crystallization temperature [℃]	MFR [g/10min]
0	127.8	15.0
1	128.9	17.1
3	129.7	17.9

Fujiyama et al. had a fundamental consideration about the relations among the relaxation time, the crystallization time and the quantity of molecular chain with crystal oriented (=thickness of the skin layer), and they showed that the longer the relaxation time and the longer the crystallization time, the thicker the skin layer[4]. Considering the result of this section, the addition of Mah-PP causes MFR to increase, viscosity to decrease and relaxation time to shorten. On the other hand, the crystallization temperature shifts to higher range and the time to start crystallizing becomes shorter. This result shows that each of the two effecting factors to the thickness of skin layer, considered by Fujiyama et al., have effects on both thickening and thinning of the skin layer. In the next section, we will subsequently discuss about the thickness of the skin layer by using micro-beam WAXD measurement.

3.2 The X-ray Structure Analysis of Injection Molding Specimen With Mah-PP Added

Figure 7 shows the WAXD patterns obtained at several positions on the MD-ND plane of the injection molding specimens with variable amount of Mah-PP addition.

The orientated diffraction profile patterns are obtained at the position of 25 μm from the surface of all molded specimens. On the other hand, we confirmed the tendency that the intensity is not quite large. It is considered that is because degree of crystallinity becomes relatively lower with rapid cooling by the mold. Subsequently the high-orientated WAXD patterns can be obtained at the position of 225 μm from the surface of all injection molded specimens regardless of the amount of Mah-PP addition. On the other hand, at the inner side within the position of 475 μm from the surface, WAXD patterns are like isotropic, therefore it suggests that low-oriented core layer is formed in those thickness area.

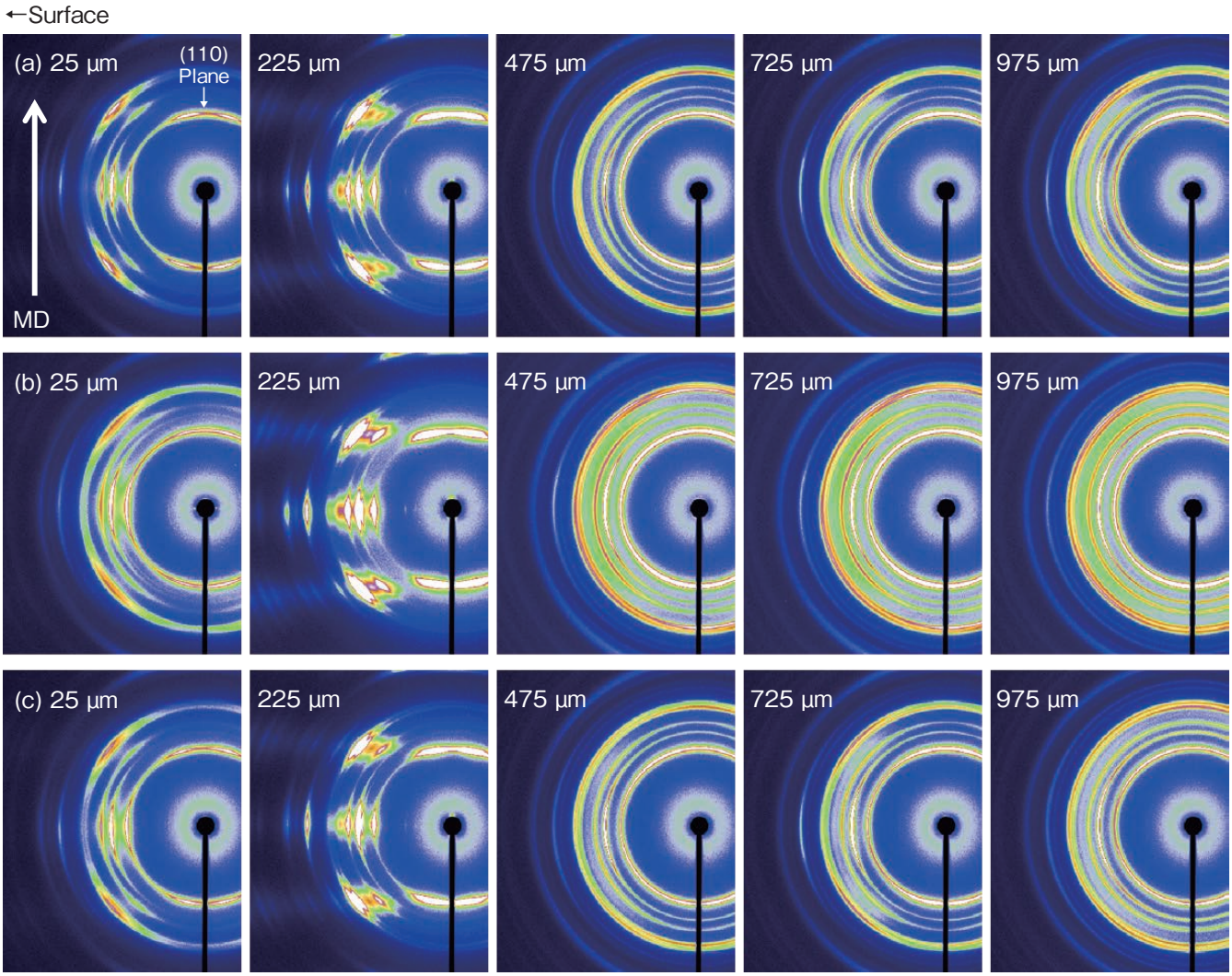

Figure 7 2D-WAXD profiles at each position from the surface of the molded sample of (a) neat PP, (b) PP/Mah-PP (1 mass%) and (c) PP/Mah-PP (3 mass%).

Next, to clarify the border between the skin layer and the core layer, the degree of orientation "fc" toward MD of c-axis is calculated from the intensity distribution in the azimuth angle direction of the PP crystal's (110) reflection obtained at each of the measurement points, and the distribution of the PP crystal orientation function in the ND direction on the MD-ND plane is calculated. The results are shown in Figure 8.

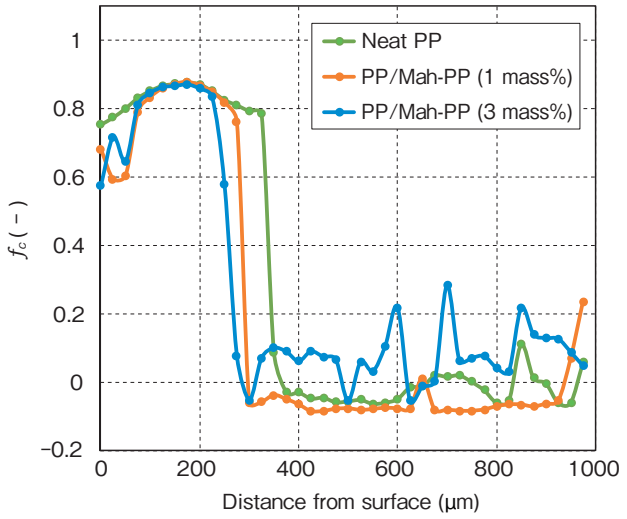

Figure 8 Orientation functions of c-axis of various samples as a function of distance from the surface.

It is found that while all molded specimens have relatively high-degree of orientation at the surface, the degree of orientation at the position of 100 μm from the surface slightly decreases because of the Mah-PP addition.

Next, we study the thickness of the skin layer from the orientation function in the thickness direction. Drastic decrease of orientation function is observed between 325 μm to 350 μm with the neat PP, therefore it is considered that there is a border of skin layer and core layer within this range. On the other hand, with the Mah-PP addition, the range where the orientation function drastically decreases shifts to the range within 275-300 μm with 1 mass% addition and within 225-275 μm with 3 mass% addition. That means that the high-oriented skin layer becomes thinner with the Mah-PP addition. It can be said that, with the Mah-PP addition, shortening relaxation time caused by viscosity decrease has more effect to the thinning of the skin layer than the effect of crystallization described in Section 3.1.

Focusing on the orientation degree in the core layer, the orientation degrees are negative values in the core layer of all molding specimens. It is considered that there is slight a-axis orientation in the core layer. On the other hand, it is confirmed the tendency that c-axis orientation function becomes slightly higher in the core layer when the Mah-PP addition is large. This is estimated that crystallization behavior and the variation of relaxation time, with the Mah-PP addition, contribute to, however the details of how such configuration occurs still remains unknown.

Next, averaging diffraction profile patterns in the direction of azimuthal angle, the degree of crystallinity estimated from the 2θ vs intensity-curve is shown in Figure 9. It is found that, comparing with neat PP, the degree of crystallinity becomes slightly higher in the surface layer and the core layer with adding the Mah-PP. As described in the Section 3.1, this is estimated that is because crystallization speed becomes faster. From the results so far, the orientation function and the degree of crystallinity in the direction of the thickness on the injection molding specimens can be analyzed in detail, and it is found that the skin layer becomes thinner with Mah-PP adding. There is the possibility that the thinning of skin layer causes decrease in the tensile modulus, therefore we discuss about the results of mechanical properties in the next section.

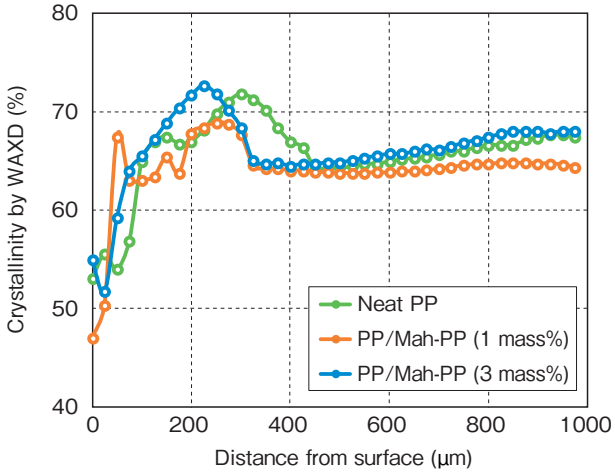

Figure 9 The degree of crystallinity for various samples as a function of the distance from surface.

3.3 The Measurements of the Strength and the Tensile Modulus of Injection Molding Specimens With the Mah-PP Addition

Table 2 shows the results of the tensile test. It is already described in Section 3.2 about the thinning of the skin layer thickness with the Mah-PP addition, however the tensile strength and the tensile modulus didn't change much even if the amount of the Mah-PP addition is increased. For the PP fiber, relationship between the orientation function and the tensile modulus of PP has been studied many times from long time ago. Shimizu et al. elucidated the relations among the drawn speed, the tensile modulus, orientation function and the birefringence of the PP fiber[6), 7)]. They show that, between the tensile modulus and birefringence, at threshold level, the effect of the tensile modulus increment in large slope is obtained toward the increase of birefringence in the high-birefringence region, however the slope of the tensile

modulus increment is small toward increment of birefringence in the low-birefringence region. From the literatures, it can be considered that birefringence and the orientation function are in a proportional relation.

Table 2 Tensile modulus and strength of neat PP an PP/Mah-PP blends.

Mah-PP content [mass%]	Tensile modulus [GPa]	Tensile strength [MPa]
0	2.1	40.8
1	2.0	39.4
3	2.1	39.5

From the results of this measurements for the mechanical properties, even though there is slight effect of thinning to thin the skin layer, it can be estimated that, the effect of low- degree orientation core layer which forms a large part of specimen's volume is larger than the effect of regions which have orientation degree sufficient to contribute to the elasticity degree, and it leads to no-large difference between bulk tensile modulus of the moldings.

On the other hand, since the thickness of skin layer has a possibility to affect the occurring warpages in use, it is considered that attention to the properties is required in the case of fiber reinforced PP composite as the original purpose of the Mah-PP adding. In the case of fiber reinforced, it is necessary to consider effects of variations of fluidity and crystallization behavior caused by the fiber addition, therefore it is necessary to verify continuously if the results of this time can be applicable or not to the materials which are filer added or fiber reinforced composite.

4. CONCLUSION

On the injection molding specimen consisting of neat PP melt-blended with Mah-PP, by observing wide angle X-ray profiles of local region in the injection molding specimen using micro-beam WAXD of SPring-8,which has a high resolution, we analyzed the degree of crystallinity and crystal orientation which occur in the molding specimen, and examined details of the degree of crystallinity and the orientation function in the thickness direction of the molding, as factors which has influence on the mechanical properties, and confirmed correlation with physical properties.

From the result, we could analyze the crystal orientation in the MD-ND plane of the injection molding specimen by micro-beam WAXD, and analyze the skin layer becomes thinner which is effected by the fluidity caused from the increment of the Mah-PP addition.

On the other hand, it is found that the Mah-PP addition has not large effect on the tensile strength and modulus, however there is possibility that variation of the skin layer's thickness of the molding effects to the long-term properties including the occurrence of sinks and warpages associated with residual stress occurring, therefore attention is required.

Recently, according to high value addition of materials, importance of core analysis technology such as structural analysis and simulation in developments is increasing more than ever. Therefore there are reports[8] about simulation technique, corresponding to more than 10^2°C/sec of the cooling rate of a skin layer in the injected molding, by utilizing equipment such as a high-speed DSC, performing high-speed crystallization analysis and associating crystallinity and oriented crystallization in the direct flow. And also an observation technique for filler dispersion and orientation under non-destruction, such as X-ray CT, and a flow analysis technique by computer aided engineering (CAE) are developed[9].

We will continue to strengthen the core analysis technique by combining this time analysis technique of crystalline orientation with those existing techniques, and utilize those techniques to the designing of plastic products.

ACKNOWLEDGEMENTS

The experiments at SPring-8 described in this study are the issues no.2016A3270, 2016B3270, 2017A3270 and 017B3270 and performed on the beamline BL24XU.

We express our sincere thanks to all people involved for providing the most cutting edge equipment and supporting system to solve technological problems in the industries.

REFERENCES

1) Manabu Nomura, Yasunobu Yamazaki, Hiroyuki Hamada: "Seikei-Kakou [Polymer Processing]", 12 (2003), 830-832. (in Japanese)
2) Kenji Aoki: "Seikei-Kakou Symposia '18 [Polymer Processing Meeting '18]", (2018), 123. (in Japanese)
3) Hiroshi Awaya: "Koubunshi [High Polymers]", 158 (1965), 379-388. (in Japanese)
4) Mitsumi Fujiyama, Syukichi Kimura: "Koubunnshi Ronbunshu [Japanese journal of polymer science and technology]", 10 (1975), 581-590. (in Japanese)
5) Yutaka Kobayashi: "Seikei-Kakou [Polymer Processing]", 4 (2016), 149-152. (in Japanese)
6) Jiro Shimizu, Kouichiro Torikai, Yoshitaka Imai: "Sen'i Gakkaishi [Journal of SFSTJ]", 6 (1977), 59-64. (in Japanese)
7) Jiro Shimizu, Tokumasa Okui, Yoshitaka Imai: "Sen'i Gakkaishi [Journal of SFSTJ]", 10 (1979), 35-42. (in Japanese)
8) Yasuhiko Otsuki, Yutaka Kobayashi, Wataru Takarada, et al.: "Seikei-Kakou Symposia '19 [Polymer Processing Meeting '19]", (2019), 189-190. (in Japanes)
9) Azusa Iida, Kazuaki Okamoto, Kouichiro Kondo, et al.: "Seikei-Kakou [Polymer Processing]", 13 (2013), 359-360. (in Japanese)